



# Winter-to-summer evolution of $p\text{CO}_2$ in surface water and air–sea $\text{CO}_2$ flux in the seasonal ice zone of the Southern Ocean

D. Nomura<sup>1,2</sup>, H. Yoshikawa-Inoue<sup>3</sup>, S. Kobayashi<sup>3</sup>, S. Nakaoka<sup>4</sup>, K. Nakata<sup>1,3</sup>, and G. Hashida<sup>5</sup>

<sup>1</sup>Institute of Low Temperature Science, Hokkaido University, Kita-19, Nishi-8, Kita-ku, Sapporo, Hokkaido 060-0819, Japan

<sup>2</sup>Japan Society for the Promotion of Science (JSPS), 6 Ichiban-cho, Chiyoda, Tokyo 102-8471, Japan

<sup>3</sup>Graduate School of Environmental Science and Faculty of Environmental Earth Science, Hokkaido University, Kita-10, Nishi-5, Kita-ku, Sapporo 060-0810, Japan

<sup>4</sup>National Institute for Environmental Studies, 16-2 Onogawa, Tsukuba, Ibaraki 305-0053, Japan

<sup>5</sup>National Institute of Polar Research, 10-3 Midori-cho, Tachikawa, Tokyo 190-8501, Japan

Correspondence to: D. Nomura (daiki@lowtem.hokudai.ac.jp)

Received: 30 November 2013 – Published in Biogeosciences Discuss.: 10 January 2014

Revised: 11 September 2014 – Accepted: 11 September 2014 – Published: 16 October 2014

**Abstract.** Partial pressure of  $\text{CO}_2$  ( $p\text{CO}_2$ ) in surface water and vertical profiles of the carbonate system parameters were measured during austral summer in the Indian sector of the Southern Ocean (64–67° S, 32–58° E) in January 2006 to understand the  $\text{CO}_2$  dynamics of seawater in the seasonal ice zone. Surface-water  $p\text{CO}_2$  ranged from 275 to 400  $\mu\text{atm}$ , and longitudinal variations reflected the dominant influence of water temperature and dilution by sea ice meltwater between 32 and 40° E and biological productivity between 40 and 58° E. Using carbonate system data from the temperature minimum layer ( $-1.9^\circ\text{C} < T < -1.5^\circ\text{C}$ ,  $34.2 < S < 34.5$ ), we examined the winter-to-summer evolution of surface-water  $p\text{CO}_2$  and the factors affecting it. Our results indicate that  $p\text{CO}_2$  increased by as much as 32  $\mu\text{atm}$ , resulting mainly from the increase in water temperature. At the same time as changes in sea ice concentration and surface-water  $p\text{CO}_2$ , the air–sea  $\text{CO}_2$  flux, which consists of the exchange of  $\text{CO}_2$  between sea ice and atmosphere, changed from  $-1.1$  to  $+0.9$   $\text{mmol C m}^{-2} \text{ day}^{-1}$  between winter and summer. These results suggest that, for the atmosphere, the seasonal ice zone acts as a  $\text{CO}_2$  sink in winter and a temporary  $\text{CO}_2$  source in summer immediately after the retreat of sea ice. Subsequent biological productivity likely decreases surface-water  $p\text{CO}_2$  and the air–sea  $\text{CO}_2$  flux becomes negative, such that in summer the study area is again a  $\text{CO}_2$  sink with respect to the atmosphere.

## 1 Introduction

The Southern Ocean is an area of a large  $\text{CO}_2$  flux between ocean and atmosphere because of its large surface area and strong regional winds (Sabine and Key, 1998). Furthermore, water formed in the Southern Ocean ventilates the intermediate and deep depths of much of the world ocean (Rintoul and Bullister, 1999). Limited seasonal observations show that the air–sea  $\text{CO}_2$  flux in the Southern Ocean varies over a wide range, reflecting its oceanographic complexity (e.g., Takahashi et al., 2009). Recently, McNeil et al. (2007) computed a total  $\text{CO}_2$  uptake of  $-0.4$   $\text{Gt C year}^{-1}$  by the Southern Ocean on the basis of  $\text{CO}_2$  partial pressure ( $p\text{CO}_2$ ) in surface water, calculated from carbonate system parameters in seawater that were parameterized separately for the summer and winter seasons as a function of temperature, salinity and nutrient levels. More recently, however, Takahashi et al. (2009) estimated a smaller  $\text{CO}_2$  uptake of  $-0.05$   $\text{Gt C year}^{-1}$  by incorporating new  $p\text{CO}_2$  data from the 2000s and from the seasonal ice zone (SIZ), where relatively high  $p\text{CO}_2$  exists in the water under the ice (Bakker et al., 1997, 2008; Rubin et al., 1998; Bellerby et al., 2004) and where the release of  $\text{CO}_2$  to the atmosphere is limited to small areas of open water (e.g., polynyas, leads and cracks) in the ice-covered area.

The SIZ is the region where sea ice covers the surface of the ocean in winter and melts in summer (Moore and Abbott, 2000). The distribution of surface-water  $p\text{CO}_2$  in the SIZ in the Southern Ocean is characterized by large variability in

space and time. In winter, both supersaturation and undersaturation of surface-water  $p\text{CO}_2$  with respect to the atmosphere has been reported (Hoppema et al., 1995; Bakker et al., 1997; Rubin et al., 1998; Gibson and Trull, 1999; Stoll et al., 1999; Bellerby et al., 2004; Metzl et al., 2006; Takahashi et al., 2009). McNeil et al. (2007) demonstrated the seasonal difference of surface-water  $p\text{CO}_2$  between winter and summer in the Southern Ocean, and both positive and negative differences were distributed inhomogeneously. These results suggest that it is difficult to characterize the seasonal and areal surface-water  $p\text{CO}_2$  distribution in SIZ.

In winter, sea ice formation and the associated release of brine to the underlying seawater is the main driver of deep water formation, and this process contributes to the formation of high- $p\text{CO}_2$  water (Nomura et al., 2006; Rysgaard et al., 2007). Respiration creates high- $p\text{CO}_2$  water during the season of low sunlight. In addition, sea ice may inhibit the release of  $\text{CO}_2$  from the sea surface to the atmosphere, leading to the accumulation of  $\text{CO}_2$  under the sea ice, although recent studies have proposed that  $\text{CO}_2$  is released directly from sea ice (Nomura et al., 2006; Miller et al., 2011; Geilfus et al., 2013). On the other hand, observations of low surface-water  $p\text{CO}_2$  during winter (e.g., Hoppema et al., 1995; Stoll et al., 1999) have been explained as a remnant of low- $p\text{CO}_2$  water formed during earlier seasons (Sweeney et al., 2000; Sweeney, 2003; Hales and Takahashi, 2004; Metzl et al., 2006; Takahashi et al., 2009). In general the literature depicts  $\text{CO}_2$  dynamics in the SIZ as a complicated subject because of the sparsity of samples and imprecision in the parameterizations for processes including eddy mixing, ice formation and melting and biological processes (Takahashi et al., 2012).

This study investigated the dynamics of  $\text{CO}_2$  in seawater and its interaction with the atmosphere on the basis of surface-water  $p\text{CO}_2$  data and the vertical profile of carbonate systems in the SIZ in the Indian sector of the Southern Ocean, measured in January (austral summer) of 2006. We used data from vertical profiles of carbonate system parameters in the temperature minimum layer to analyze changes in the surface-water  $p\text{CO}_2$  and evaluate their relation to  $p\text{CO}_2$  dynamics of the surface water and air–sea  $\text{CO}_2$  flux.

## 2 Methods

We sampled from the R/V *Umitaka-Maru* in the Indian sector of the Southern Ocean (64–67° S, 32–58° E) from 12 to 19 January 2006 (Fig. 1 and Table 1). Stations L1–8 were far from the coast, and station FG3 was near the coast of Antarctica (Fig. 1).

During the cruise,  $p\text{CO}_2$  in surface water was evaluated through the underway water measuring system (Inoue and Ishii, 2005; Nakaoka et al., 2009).  $\text{CO}_2$  concentration (mole fraction of  $\text{CO}_2$  in dry air;  $x\text{CO}_2$ ) was measured quasi-continuously in the air equilibrated with seawater using an automated  $\text{CO}_2$  measuring system (Nippon ANS Co. Ltd.,

Tokyo, Japan). This system consisted of a unit for the removal of water vapor in sample air (a chemical desiccant column ( $\text{Mg}(\text{ClO}_4)_2$ ) and an electric dehumidifier). Seawater was taken continuously from a depth of about 10 m and introduced into the shower-type equilibrator (Inoue and Ishii, 2005). A non-dispersive infrared gas analyzer (Model 800, LI-COR, Inc., Lincoln, NE, USA) was used as the detector for  $\text{CO}_2$  concentration measurements. The analyzer was calibrated every 1 h with four  $\text{CO}_2$  standards (200, 266, 320 and 400 ppm) traceable to the World Meteorological Organization mole fraction scale (Inoue and Ishii, 2005). For measurements of atmospheric  $\text{CO}_2$  concentration, air samples were pumped through a Teflon tube from the ship's mast and introduced to the  $\text{CO}_2$  analyzer every 6 min.  $p\text{CO}_2$  was calculated from  $x\text{CO}_2$  taking into account the saturated water vapor pressure and atmospheric pressure. The precision of  $p\text{CO}_2$  measurements was less than  $2 \mu\text{atm}$ , as estimated on the basis of the uncertainty of the rise in seawater temperature between the surface and a non-dispersive infrared gas (NDIR) analyzer ( $1 \mu\text{atm}$ ). The rise of seawater temperature between the surface and the equilibrator was typically  $1.7^\circ\text{C}$ , and the effect of the seawater temperature rise on the measured value of  $p\text{CO}_2$  was corrected using the isochemical temperature dependence of  $p\text{CO}_2$  given by Copin-Montegut (1988).

Sea surface temperature (SST) and salinity (SSS) were measured continuously with a CT sensor (Falmouth Scientific, Inc., Cataumet, MA, USA). The accuracy of temperature and salinity is  $\pm 0.005^\circ\text{C}$  and  $\pm 0.001$ , respectively. Seawater samples were taken in order to calibrate the salinity sensor. Sea surface fluorescence was measured with a fluorescence probe (WETStar, WETLabs Inc., Philomath, OR, USA) at an inlet of the equilibrator. The sensitivity of this probe is  $0.03 \mu\text{g L}^{-1}$  (<http://www.wetlabs.com/content/wetstar>). The fluorescence was converted to the chlorophyll *a* concentration based on the relationships between fluorescence and chlorophyll *a* concentration determined by a fluorometer (Model 10AU, Turner Designs, Inc., Sunnyvale, CA, USA) for the same water sample. The detection limit of this fluorometer is  $0.025 \mu\text{g L}^{-1}$  (<http://www.turnerdesigns.com/products/laboratory-fluorometer/10au-laboratory-fluorometer>).

Vertical profiles of temperature and salinity were measured with a conductivity–temperature–depth (CTD) probe (SBE 911 plus, Sea-Bird Electronics, Bellevue, WA, USA) that was calibrated by the manufacturer before and after the cruise. In addition, seawater samples were taken to calibrate the salinity sensor. Seawater samples were collected vertically (0, 10, 20, 30, 50, 75, 100, 150, 200 and 500 m) in rosette-mounted 2.5 L Niskin bottles (Ocean Test Equipment, Inc., Lauderdale, FL, USA). Seawater was subsampled into a 120 mL amber glass vial (Maruemu Co., Ltd., Osaka, Japan) for the determination of dissolved inorganic carbon (DIC) and total alkalinity (TA) and into a 500 mL Nalgene polycarbonate bottle (Thermo Fisher Scientific, Inc., Waltham, MA, USA) for the determination of chlorophyll *a* concentration.

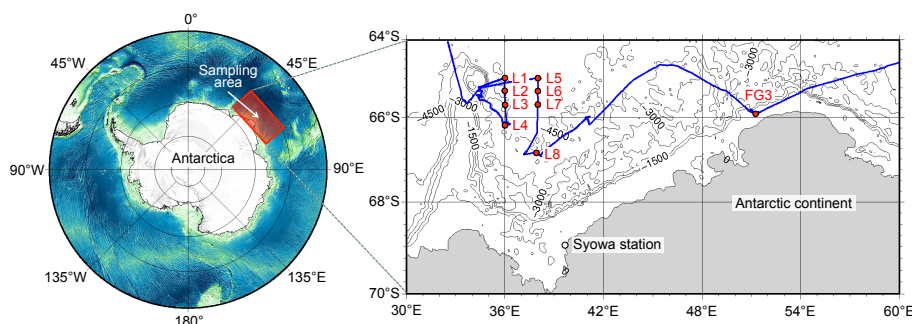


**Figure 1.** Location map of the sampling area in the Indian sector of the Southern Ocean showing the cruise track (blue line) and CTD station locations (red circles). Bathymetric contours are at 750 m intervals.

**Table 1.** Sampling dates, times (UTC) and locations of CTD stations.

Station	Date in 2006	Time	Latitude (° S)	Longitude (° E)
L1	13 January	10:23	65.0	36.0
L2	13 January	03:31	65.3	36.0
L3	12 January	22:25	65.7	36.0
L4	12 January	03:49	66.2	36.0
L5	14 January	16:59	65.0	38.0
L6	14 January	22:36	65.3	38.0
L7	15 January	03:41	65.7	38.0
L8	16 January	03:30	66.9	37.9
FG3	19 January	07:19	65.9	51.4

Immediately after DIC and TA sampling, a saturated mercury chloride ( $\text{HgCl}_2$ ) solution ( $100\ \mu\text{L}$ ) was added to stop biological activity. Samples for the measurement of DIC and TA were stored in a refrigerator at  $+4\ ^\circ\text{C}$  until analysis. Samples for chlorophyll  $a$  measurement were immediately filtered through 25 mm Whatman GF/F filters, and filters were stored in a deep freezer ( $-80\ ^\circ\text{C}$ ) until analysis (Suzuki and Ishimaru, 1990). Chlorophyll  $a$  concentration was determined by fluorometry (Parsons et al., 1984).

DIC was determined by coulometry (Johnson et al., 1999) using a coulometer (CM5012, UIC, Inc., Binghamton, NY, USA). The precision of DIC analysis from duplicate determinations is within  $\pm 0.1\ \%$  (Wakita et al., 2003). TA was determined by the improved single-point titration method (Culbertson et al., 1970) using a pH meter (PHM240, Radiometer Analytical, Lyon, France). The precision of the TA analysis from duplicate determinations is within  $\pm 0.2\ \%$  (Wakita et al., 2003). Measurements for DIC and TA were calibrated by using the certified reference material distributed by the A. G. Dickson of Scripps Institution of Oceanography. To correct for the effect of dilution on DIC and TA due to the melting of sea ice during the winter-to-summer transition, DIC and TA data were normalized ( $n\text{-DIC}$  and  $n\text{-TA}$ ) to a salinity of 34.25, the mean value of the temperature mini-

um layer (TML). Tomczak and Liefink (2005) proposed that a water mass beneath the summer surface water with a temperature between  $-1.9$  and  $-1.5\ ^\circ\text{C}$  and a salinity between 34.2 and 34.5 constitutes the TML, and the TML is thought to retain the winter condition. Therefore, we used a salinity of 34.25 for the normalization of DIC and TA data as an initial condition before the change by the input of ice meltwater.

Satellite images of sea ice concentration near sampling stations were derived from passive microwave imagery from the Advanced Microwave Scanning Radiometer–Earth Observing System (AMSR-E) (<http://nsidc.org/data/amsre>; the Level-3 gridded product (AE\_SI12) was downloaded from [http://nsidc.org/data/ae\\_si12](http://nsidc.org/data/ae_si12)). Spatial resolution was a  $12.5\ \text{km} \times 12.5\ \text{km}$  grid, and temporal resolution was 1 day; we used 8-day averages of data in this study. For deriving sea ice concentrations, we used the enhanced NASA Team (NT2) algorithm.

Satellite images of the chlorophyll  $a$  concentration near our sampling stations were derived from Sea-viewing Wide Field-of-view Sensor (SeaWiFS) data from NASA (<http://oceancolor.gsfc.nasa.gov/SeaWiFS/>), specifically the standard Level-3 products of 8-day composite SeaWiFS chlorophyll concentration data. We derived chlorophyll  $a$  concentrations with the OC4 chlorophyll  $a$  algorithm (O'Reilly et al., 2000) (<http://oceancolor.gsfc.nasa.gov/REPROCESSING/R2009/ocv6/>). Spatial resolution was a  $9\ \text{km} \times 9\ \text{km}$  grid, and temporal resolution was 1 day; we used 8 days of composite data in this study. Cannizzaro et al. (2013) compared chlorophyll  $a$  data from in situ and SeaWiFS measurements and found that they were highly correlated ( $r^2 = 0.84$ ,  $n = 289$ ) although SeaWiFS values were positively biased by 25 %.

### 3 Results

#### 3.1 Longitudinal distribution of $p\text{CO}_2$ , SST, SSS and chlorophyll $a$ concentration

Surface-water  $p\text{CO}_2$  ranged from 275 to 399  $\mu\text{atm}$ , and mean air  $p\text{CO}_2$  was  $366.2 \pm 4.0 \mu\text{atm}$  (mean  $\pm 1$  SD) (Fig. 2a). Most  $p\text{CO}_2$  in surface water was undersaturated with respect to the atmosphere in the area between 38 and 58° E. Surface-water  $p\text{CO}_2$  decreased from 399  $\mu\text{atm}$  at 36–37° E to 275  $\mu\text{atm}$  at 44° E and then increased to 340  $\mu\text{atm}$  at 58° E. Chlorophyll  $a$  concentrations ranged from 0.2 to 0.9  $\mu\text{g L}^{-1}$  (Fig. 2b), reaching their maximum at 42.5° E. SST ranged from  $-1.5$  to  $+1.2^\circ\text{C}$  and was generally low in the areas of 33–40 and 45–58° E (Fig. 2c). SSS ranged from 32.5 to 34.1, reaching its minimum at 39° E (Fig. 2d).

#### 3.2 Satellite images of sea ice and chlorophyll $a$ concentrations

Temporal images of the sea ice concentration near sampling stations were shown in Fig. 3. Before the middle of December 2005, the area near the sampling stations was  $> 80\%$  covered by sea ice (Fig. 3a). In the middle and at the end of December 2005, sea ice areas decreased from north to south (Fig. 3b–d). Sea ice was absent north of stations L1–8 in the middle of January 2006 (Figs. 3e, f and 4a). Sea ice just reached its minimum before disappearing in the summer in the middle of March 2006 (Fig. 3g). For station FG3, sea ice concentration began to decrease in early November 2005 and covered less than 80% of the surface until the middle of December, when coverage grew again to 80% (Fig. 4a). The sea ice minimum occurred later here (end of February) than at the other stations (middle of January) (Fig. 4a).

Temporal images of the chlorophyll  $a$  concentration near our sampling stations were shown in Fig. 5. After sea ice had retreated, chlorophyll  $a$  concentrations near sampling stations increased, particularly near the ice edge (Figs. 4 and 5). At station FG3, a rapid increase of chlorophyll  $a$  was observed in early February (Fig. 4b). At the other stations, chlorophyll  $a$  concentration remained constant from January to March 2006.

#### 3.3 Vertical profiles of temperature, salinity, $n$ -DIC, $n$ -TA and chlorophyll $a$ concentration

For stations L1–8, vertical temperature profiles indicated higher temperatures above a 30 and below a 100 m depth and lower temperatures between these depths (Fig. 6a). Salinity was low in the top 30 m, particularly at station L8 (32.5), and increased up to 34.7 with depth (Fig. 6b). The TML was at a 50 m depth at stations L1–8 and at 200 m at station FG3 (Fig. 6).

The  $n$ -DIC was almost constant in the top 50 m of the water column (1 SD =  $\pm 4 \mu\text{mol kg}^{-1}$ ) (although different at each station), then increased down to a 100 m depth (Fig. 6c).

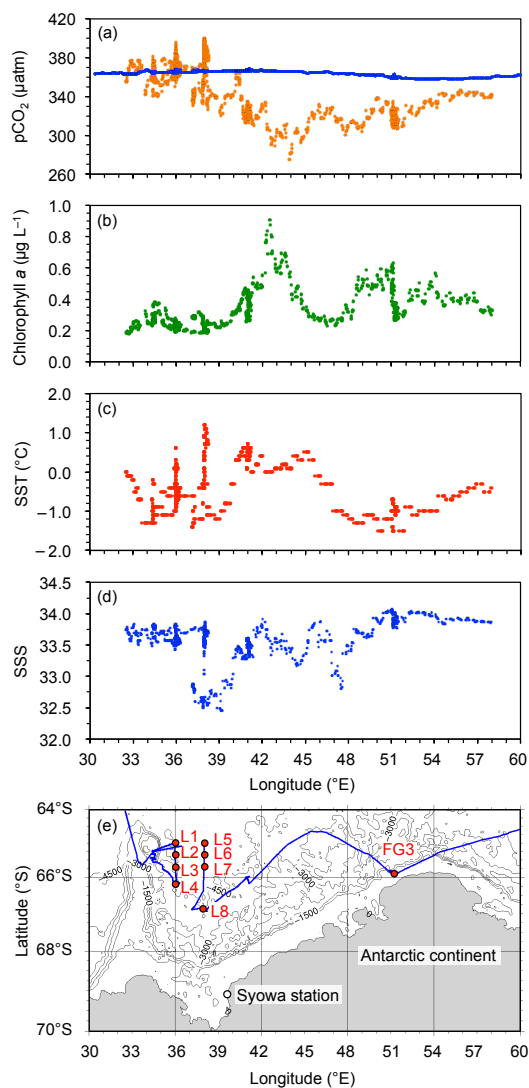


**Figure 2.** Longitudinal distribution of surface-water  $p\text{CO}_2$  (a), chlorophyll  $a$  (b), SST (c), SSS (d) and location map (e). Blue line in (a) indicates atmospheric  $p\text{CO}_2$ .

The  $n$ -TA decreased slightly with depth (Fig. 6d). Chlorophyll  $a$  concentration was low at the surface and below a 130 m depth although some stations had peaks up to  $1.0 \mu\text{g L}^{-1}$  deeper than 50 m (Fig. 6e).

For station FG3, near the coast of Antarctica, vertical profiles showed lower temperature, salinity and  $n$ -DIC and higher chlorophyll  $a$  concentration than at stations L1–8 (Fig. 6). For  $n$ -TA, profiles at all stations were similar (Fig. 6d).

### 4 Discussion

The longitudinal distribution of  $p\text{CO}_2$  in surface water varies with environmental factors. To understand the fac-

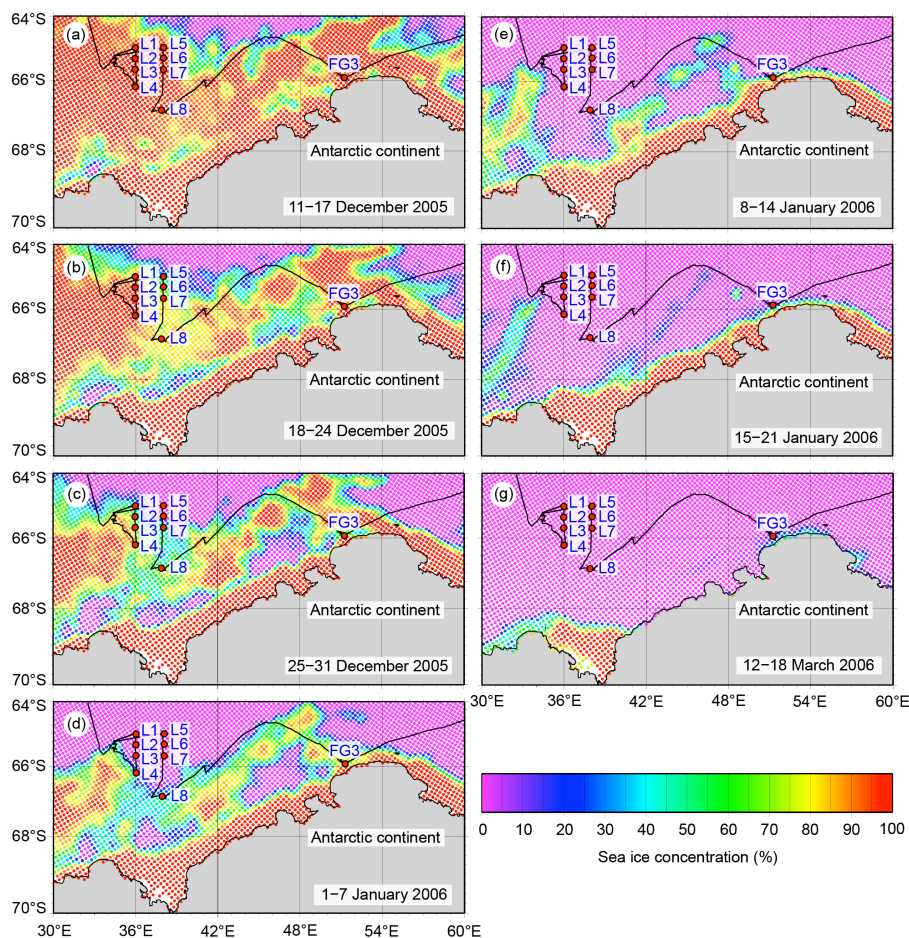


**Figure 3.** Seasonal variation in sea ice concentration in the study area for 11–17 (a), 18–24 (b), 25–31 December 2005 (c), 1–7 (d), 8–14 (e), 15–21 January 2006 (f) and 12–18 March 2006, representing the annual minimum ice cover (g). Images derived from AMSR-E satellite data.

tors controlling surface-water  $p\text{CO}_2$ , we compared the  $p\text{CO}_2$  distribution with chlorophyll  $a$ , SST and SSS. The chlorophyll  $a$  concentration was low ( $0.2 \pm 0.0 \mu\text{g L}^{-1}$ ) (mean  $\pm 1$  SD) (median =  $0.2 \mu\text{g L}^{-1}$ ) between  $32$  and  $40^\circ \text{E}$  and relatively high ( $0.4 \pm 0.1 \mu\text{g L}^{-1}$ ) (median =  $0.4 \mu\text{g L}^{-1}$ ) between  $40$  and  $58^\circ \text{E}$  (Fig. 2b). Figure 7 compares surface-water  $p\text{CO}_2$  with SST for longitudes  $32$ – $40$ ,  $38$ – $40$  (an area strongly affected by meltwater dilution) and  $40$ – $58^\circ \text{E}$ . At  $32$ – $40^\circ \text{E}$ , the increase in surface-water  $p\text{CO}_2$  with SST was  $14.4 \mu\text{atm } ^\circ\text{C}^{-1}$ , or  $3.9 \% ^\circ\text{C}^{-1}$  (Fig. 7a); this is close to the previously estimated value of  $4.2 \% ^\circ\text{C}^{-1}$  due to thermodynamic effects (Takahashi et al., 2002). For the area affected by freshwater input, particularly at  $37$ – $40^\circ \text{E}$  (Fig. 2d),  $p\text{CO}_2$  decreased due to dilution by meltwater from sea ice (Fig. 7b) although surface-water  $p\text{CO}_2$  was also dependent on SST ( $4.6 \% ^\circ\text{C}^{-1}$ ). In  $40$ – $58^\circ \text{E}$  (Fig. 7c), there was no significant relationship between surface-water  $p\text{CO}_2$  and SST. In this biologically productive area,  $p\text{CO}_2$  in surface water was apparently strongly affected by biological processes.

Previous studies in spring and summer have reported both undersaturation of surface-water  $p\text{CO}_2$  with respect to the atmosphere (Rubin et al., 1998; Metzl et al., 1999, 2006; Chierici et al., 2004; Inoue and Ishii, 2005) and supersaturation (Bakker et al., 1997, 2008; Jabaud-Jan et al., 2004; Shim et al., 2006). Ishii et al. (2002) reported that surface-water  $p\text{CO}_2$  changed from supersaturation to undersaturation with respect to the atmosphere after the retreat of sea ice near our study area. Bakker et al. (2008) observed the same transition in the Weddell Gyre as retreating sea ice gave way to biologically productive water.

The TML is thought to retain the chemical characteristics of the surface mixed layer in winter (Ishii et al., 1998, 2002; Rubin et al., 1998; Hoppema and Goeyens, 1999; Pondaven et al., 2000). In the TML, carbonate system parameters were nearly identical at all stations ( $2207 \pm 2 \mu\text{mol kg}^{-1}$  for  $n\text{-DIC}$ ,  $2328 \pm 2 \mu\text{mol kg}^{-1}$  for  $n\text{-TA}$ ), and we treated these values as representative of winter conditions ( $n\text{-DIC}_{(w)}$  and  $n\text{-TA}_{(w)}$ ). Surface-water  $p\text{CO}_2$  in winter ( $p\text{CO}_{2w(w)}$ ) was computed from  $n\text{-DIC}_{(w)}$  and  $n\text{-TA}_{(w)}$  at the freezing

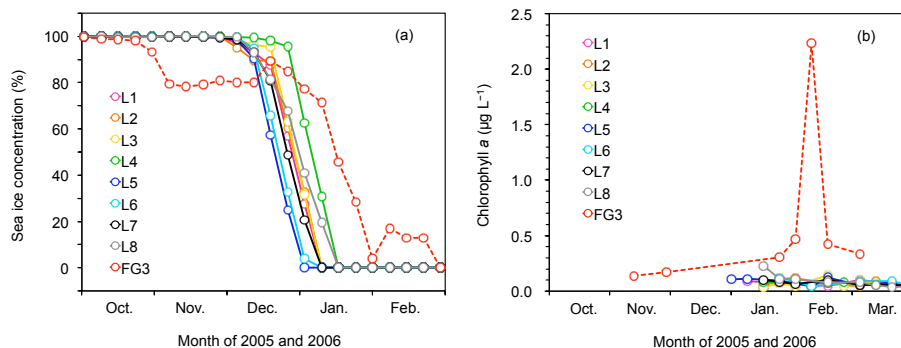


**Figure 4.** Seasonal variations in sea ice concentration from AMSR-E data (a) and chlorophyll *a* concentration from SeaWiFS data (b).

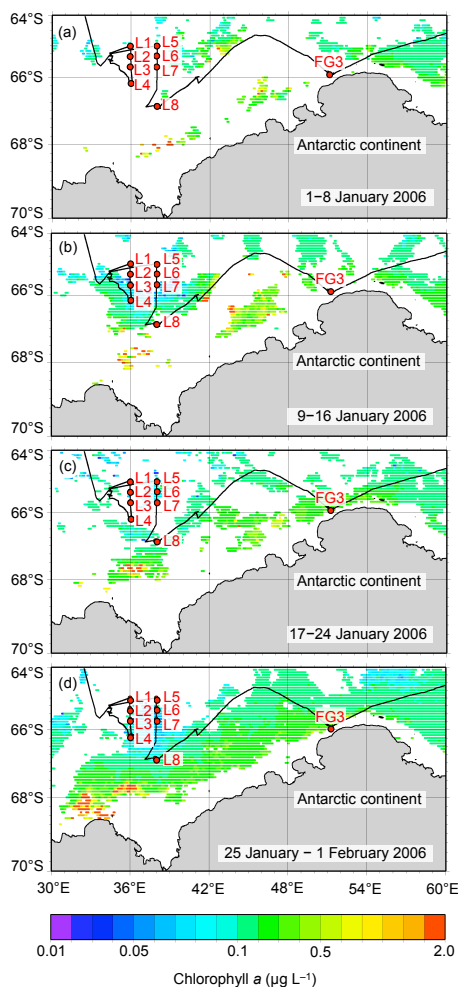


**Figure 5.** Seasonal variation in chlorophyll *a* concentration in the study area for 1–8 (a), 9–16 (b), 17–24 January (c) and 25 January–1 February (d) from SeaWiFS imagery. White area indicates no data due to the presence of sea ice or clouds.

temperature of  $-1.8\text{ }^{\circ}\text{C}$  using the program CO2SYS, version 01.05 (Lewis and Wallace, 1998). We used the carbonate dissociation constants ( $K_1$  and  $K_2$ ) of Mehrbach et al. (1973) as

revised by Dickson and Millero (1987) and the  $K_{\text{SO}_4}$  determined by Dickson (1990). The resulting value of  $p\text{CO}_{2\text{w(w)}}$  was  $349.9 \pm 6.4\text{ }\mu\text{atm}$ , which agrees well with the  $p\text{CO}_2$  in winter derived from  $p\text{CO}_2$ –SST relationship (Fig. 7a).

Carbonate system parameters are changed by various processes, including biological (photosynthesis and respiration), gas exchange ( $\text{CO}_2$  release and uptake) and carbonate mineral dissolution and formation (Anderson and Sarmiento, 1994; Zeebe and Wolf-Gladrow, 2001). A plot of  $n$ -DIC against  $n$ -TA in water above the TML (Fig. 8) suggests a complex mix of these processes. Stations L1 and FG3 appear to be governed by biological or gas exchange processes. The data establish regression lines with a slope of  $-0.1$  for station L1 and  $-0.5$  for station FG3, which are similar to those for biological (slope =  $-0.14$ ) and gas exchange (slope =  $0$ ) processes. The decreasing of  $n$ -DIC from TML during winter to summer transition (Fig. 8) would reflect photosynthesis or a  $\text{CO}_2$  release. The areas around these stations (Stations L1 and FG3) were characterized by rapid ice melting and retreat (Figs. 3 and 4a), thereby starting gas exchange at the air–sea interface and promoting biological productivity at the ocean surface (Figs. 4 and 5). High chlorophyll *a* concentrations in vertical profiles (Fig. 6e) also reflected high biological productivity at the surface, particularly for station FG3.

For station L8, the slope of the regression line is  $1.7$  (Fig. 8), similar to that of the carbonate mineral process (slope =  $2.0$ ) for the precipitation of ikaite ( $\text{CaCO}_3 \cdot 6\text{H}_2\text{O}$ ) during sea ice formation (Dieckmann et al., 2008; Nomura et al., 2013b) and its dissolution during the ice melting season (Rysgaard et al., 2013). The increase of  $n$ -TA from TML during winter-to-summer transition (Fig. 8) would reflect ikaite dissolution during the ice melting season.

The low salinity ( $32.5$ ) at station L8 at the surface (Fig. 6b) is clear evidence of the influence of meltwater. Based on the change in salinity from  $34.25$  in winter to  $32.5$  in summer in the upper  $20\text{ m}$  of the water column, we calculate that sea ice thickness was  $1\text{ m}$ . The amount of ikaite in Antarctic sea ice has been estimated to be  $100\text{--}900\text{ }\mu\text{mol kg}^{-1}$  ice (Rysgaard et al., 2013). Under the assumption that all ikaite in sea ice is dissolved in sea ice and that meltwater is supplied to the

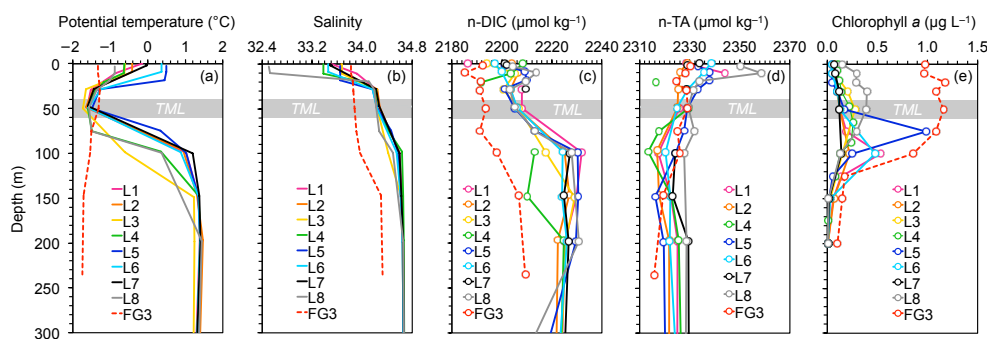


**Figure 6.** Vertical profiles of potential temperature (a), salinity (b), salinity-normalized DIC ( $n\text{-DIC}$ ) (c), salinity-normalized TA ( $n\text{-TA}$ ) (d) and chlorophyll  $a$  concentration (e). Shaded area indicates the temperature minimum layer (TML) for stations L1–8. For FG3, the TML was at 200 m.

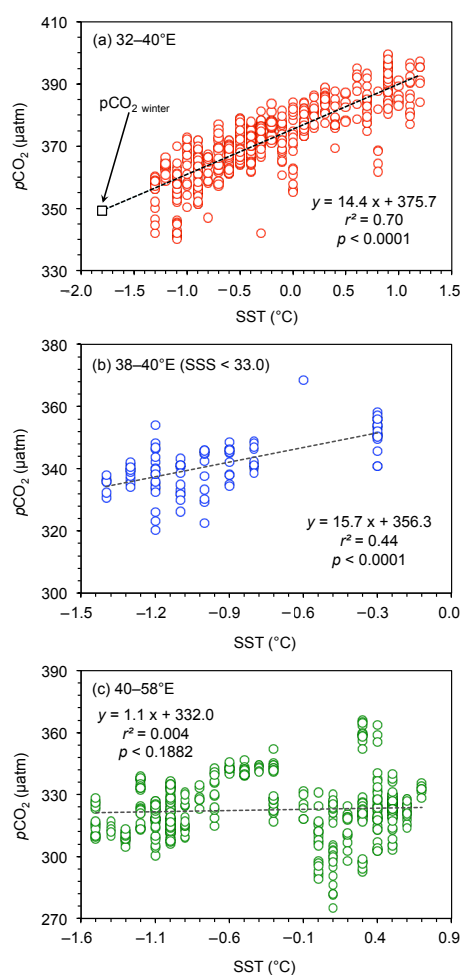


**Figure 7.** Relationship between surface-water  $p\text{CO}_2$  and SST for 32–40° E (a), the area affected by freshwater input (SSS < 33.0) in 38–40° E (b) and 40–58° E (c). Dashed lines are best-fit lines described by the regression equations. The black square in (a) indicates surface-water  $p\text{CO}_2$  in winter (349.9 μatm), calculated from the carbonate system parameters in the TML.

upper 20 m of the winter water column, the meltwater input should alter  $n\text{-DIC}$  from 2206.6 to 2211.6–2251.6 μmol kg<sup>-1</sup> and  $n\text{-TA}$  from 2327.6 to 2337.6–2417.6 μmol kg<sup>-1</sup> during the transition from winter to summer at station L8. These  $n\text{-DIC}$  and  $n\text{-TA}$  variations correspond to a  $p\text{CO}_2$  decrease from 380.7 to 300.3–370.0 μatm at constant salinity (34.25), temperature (0 °C) and barometric pressure (1 atm), as calculated using the program CO2SYS. Our estimate is consistent with ikaite formation and dissolution, which has been proposed as a contributor to changes in carbonate system parameters during the ice melt season (Fransson et al., 2011; Rysgaard et al., 2013). For the remaining stations (L2 and L4–7), a complex mixture of processes appears to be operating (Fig. 8).

We calculated the winter-to-summer evolution of surface-water  $p\text{CO}_2$  in terms of four factors in the following equation (Bakker et al., 1997; Shim et al., 2006):

$$\Delta p\text{CO}_{2w(w \text{ to } s)} = (\Delta p\text{CO}_{2w})T + (\Delta p\text{CO}_{2w})F + (\Delta p\text{CO}_{2w})B + (\Delta p\text{CO}_{2w})R, \quad (1)$$

where  $\Delta p\text{CO}_{2w(w \text{ to } s)}$  is the  $p\text{CO}_2$  change from winter (349.9 μatm) to summer (observed  $p\text{CO}_2$ ),  $(\Delta p\text{CO}_{2w})T$  is the  $p\text{CO}_2$  change from the temperature effect,  $(\Delta p\text{CO}_{2w})F$  is the  $p\text{CO}_2$  change due to air–sea  $\text{CO}_2$  flux,  $(\Delta p\text{CO}_{2w})B$  is the  $p\text{CO}_2$  change from biological activity and  $(\Delta p\text{CO}_{2w})R$  is a residual term mainly reflecting upwelling, mixing and variability of water masses including carbonate mineral dissolution/formation.

For the first term, we calculated the dependence of temperature on surface-water  $p\text{CO}_2$  for each week and then summed these for the period from winter to summer:

$$(\Delta p\text{CO}_{2w})T = \Sigma(d p\text{CO}_{2w}/dt)T, \quad (2)$$

where  $(d p\text{CO}_{2w}/dt)T$  was evaluated from the following equations (Takahashi et al., 2002):

$$(d p\text{CO}_{2w}/dt)T = p\text{CO}_{2w}(t1) - p\text{CO}_{2w}(t0), \quad (3)$$

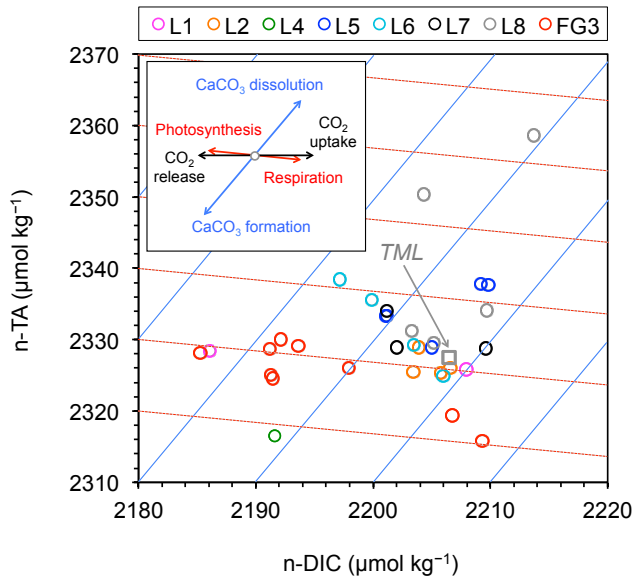


**Figure 8.** Relationships between the salinity-normalized DIC ( $n$ -DIC) and salinity-normalized TA ( $n$ -TA) for water samples shallower than the TML. The inset indicates theoretical slopes of the different processes affecting  $n$ -DIC and  $n$ -TA. Blue and red lines indicate theoretical slopes for  $\text{CaCO}_3$  dissolution/formation and photosynthesis/respiration, respectively. The gray square indicates  $n$ -DIC and  $n$ -TA in the TML.

$$p\text{CO}_{2w}(t_1) = p\text{CO}_{2w}(t_0) \cdot \exp[0.0423(Tt_1 - Tt_0)]. \quad (4)$$

In these equations,  $t$  is time ( $t_0 < t_1$ ) and  $T$  is the temperature of seawater in the  $1^\circ \times 1^\circ$  grid of optimal interpolation analysis data from Reynolds et al. (2002).

For the second term, we calculated the dependence of air–sea  $\text{CO}_2$  flux on  $p\text{CO}_2$  for every week and then summed these for the period from winter to summer:

$$(\Delta p\text{CO}_{2w})F = \Sigma(dp\text{CO}_{2w}/dt)F, \quad (5)$$

where  $(dp\text{CO}_{2w}/dt)F$  was evaluated as follows (Bakker et al., 1997):

$$(dp\text{CO}_{2w}/dt)F = \beta \cdot p\text{CO}_{2w}(F_{\text{CO}_{2(a-w)}}/\text{TDIC}), \quad (6)$$

where  $\beta$  is the buffer factor (we used the value of 14 from Takahashi et al., 1993),  $F_{\text{CO}_{2(a-w)}}$  is the  $\text{CO}_2$  flux between air and water, and TDIC is the total amount of DIC between the surface and the top of the TML. To calculate  $F_{\text{CO}_2}$ , we used the following equation:

$$F_{\text{CO}_{2(a-w)}} = k \cdot s(p\text{CO}_{2a} - p\text{CO}_{2w}) \cdot (100 - A)/100, \quad (7)$$

$$k = 0.26u^2(\text{Sc}/660)^{-0.5}, \quad (8)$$

where  $k$  is the gas transfer velocity (Wanninkhof, 1992; Takahashi et al., 2009),  $s$  is the gas solubility (Weiss, 1974),

$p\text{CO}_{2a}$  is the atmospheric  $p\text{CO}_2$  ( $366 \mu\text{atm}$ ),  $A$  is the sea ice concentration,  $u$  is the wind speed from NCEP (National Centers for Environmental Prediction) reanalysis (Kalnay et al., 2006) and  $\text{Sc}$  is the Schmidt number (Wanninkhof, 1992). There are differing opinions regarding the parameterization of the gas exchange process in the polar ocean (Ho et al., 2006; Edson et al., 2011). In this study, observational data were obtained from the open ocean and we assumed that sea ice may or may not act as an insulator under the normal water condition. Therefore, we used the parameterization of Wanninkhof (1992) in this study.

For the third term, we calculated the contribution of the biological effect on surface-water  $p\text{CO}_2$  for the period from winter to summer:

$$(\Delta p\text{CO}_{2w})B = -\beta \cdot p\text{CO}_{2w(w)}(\text{NCP}/\text{TDIC}), \quad (9)$$

where  $p\text{CO}_{2w(w)}$  is winter  $p\text{CO}_2$  in surface water ( $349.9 \mu\text{atm}$ ) and NCP is the net community production, evaluated as follows:

$$\text{NCP} = - \int_0^{Z_{\text{TMin}}} [(n\text{-DIC}(z)) - n\text{-DIC}_{\text{TML}} S(z)\rho(z)/34.25]dz, \quad (10)$$

where  $Z_{\text{Tmin}}$  is the depth of the top of the TML,  $n\text{-DIC}(z)$  is the value of  $n\text{-DIC}$  at depth  $z$ ,  $n\text{-DIC}_{\text{TML}}$  is the value of  $n\text{-DIC}$  in the TML, and  $S(z)$  and  $\rho(z)$  are, respectively, the salinity and density of seawater at depth  $z$ .

Table 2 summarizes the resulting contributions of temperature, air–sea gas exchange and biological effects on the winter-to-summer evolution of surface-water  $p\text{CO}_2$  for each station. Between winter and summer, the surface-water  $p\text{CO}_2$  for stations L1–8 increased by 15.4 to 42.0  $\mu\text{atm}$  (positive  $\Delta p\text{CO}_{2w(w \text{ to } s)}$ ), and the contribution of temperature was dominant (30.4–40.9  $\mu\text{atm}$ ). Surface-water  $p\text{CO}_2$  for station FG3 decreased by 13.2  $\mu\text{atm}$  (negative  $\Delta p\text{CO}_{2w(w \text{ to } s)}$ ), and biological production was the greatest contributor ( $-23.8 \mu\text{atm}$ ) for negative  $\Delta p\text{CO}_{2w(w \text{ to } s)}$ . The NCP value ( $13.5 \text{ g C m}^{-2}$ ) at station FG3 was the highest among all stations, supporting this result. The high chlorophyll  $a$  concentrations near station FG3 (Figs. 2b, 4b and 5) are also consistent with this result. A previous study reported even higher NCP values, up to  $34 \text{ g C m}^{-2}$ , in this area in February (Ishii et al., 1998). Station L8 had a smaller value of  $\Delta p\text{CO}_{2w(w \text{ to } s)}$  (15.4  $\mu\text{atm}$ ) than stations L1–7, and there the contribution of the fourth, residual factor was especially high. Given the low salinity of surface water at station L8 (Fig. 6b), we believe that the residual factor mainly reflects the effects of meltwater containing carbonates on surface-water  $p\text{CO}_2$ .

Taken together, our results suggest that the seasonal increase of surface-water  $p\text{CO}_2$  is mainly caused by the increase in water temperature from winter to summer in the area of stations L1–8 (Table 2). For station FG3, biological productivity is the dominant factor (Table 2). Figure 9

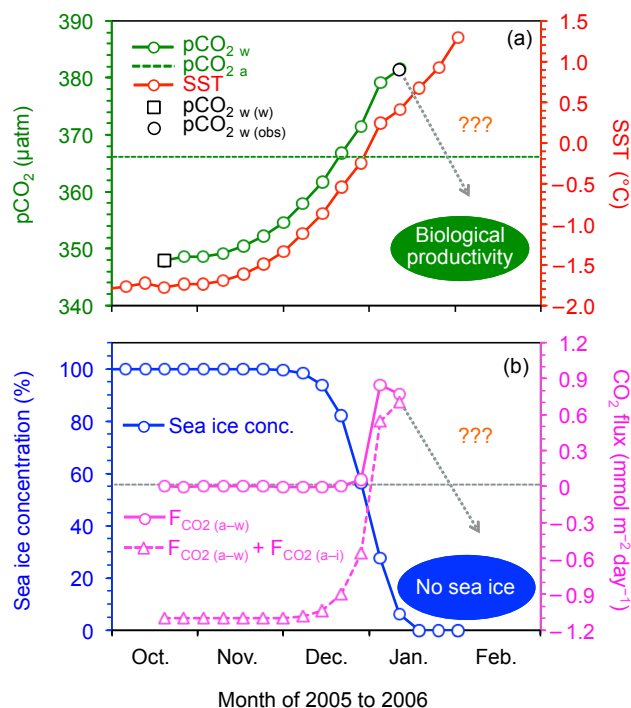


**Figure 9.** Seasonal variations of simulated surface-water  $p\text{CO}_2$  and SST (a) and sea ice concentration and  $\text{CO}_2$  fluxes (b). Simulated  $p\text{CO}_2$  in (a) is constrained by the value in winter ( $349.9 \mu\text{atm}$ ) calculated from carbonate system parameters in the TML (black square) and the value observed during our observation period ( $381.5 \mu\text{atm}$ ) (black circle).

is a graph of the calculated seasonal relationships between parameters in the SIZ in our study area as represented by stations L1–8. With the summer rise in SST, surface-water  $p\text{CO}_2$  rises above atmospheric levels in late December (Fig. 9a). Although we did not document it during our observation period, biological productivity in the study area should increase, as we observed at station FG3 (Figs. 4b, 5, 6e), after the retreat of sea ice (Fig. 9b). This development would trigger the depression of surface-water  $p\text{CO}_2$  reported by Ishii et al. (1998) and Bakker et al. (2008).

We examined the longitudinal distribution of  $p\text{CO}_2$  (Fig. 2a) to evaluate the thermodynamic dependence of surface-water  $p\text{CO}_2$  in the study area (Fig. 10), using the difference between calculated and observed  $p\text{CO}_2$  ( $p\text{CO}_{2\text{cal}} - p\text{CO}_{2\text{obs}}$ ). We computed  $p\text{CO}_{2\text{cal}}$  from  $n\text{-DIC}_{(w)}$  and  $n\text{-TA}_{(w)}$  at the observed SST and SSS using the program CO2SYS. Thus,  $p\text{CO}_{2\text{cal}}$  indicates only the thermodynamic effect on surface-water  $p\text{CO}_2$ . Therefore, the difference between  $p\text{CO}_{2\text{cal}}$  and  $p\text{CO}_{2\text{obs}}$  reflects other effects (e.g., biological effects) on surface-water  $p\text{CO}_2$  from winter to summer. This difference was near zero ( $+0.5 \pm 7.5 \mu\text{atm}$ ) between  $32$  and  $40^{\circ}\text{E}$  and as large as  $+100 \mu\text{atm}$  ( $+47.5 \pm 16.3 \mu\text{atm}$ ) between  $40$  and  $58^{\circ}\text{E}$  (Fig. 10). These results suggest that the thermodynamic ef-

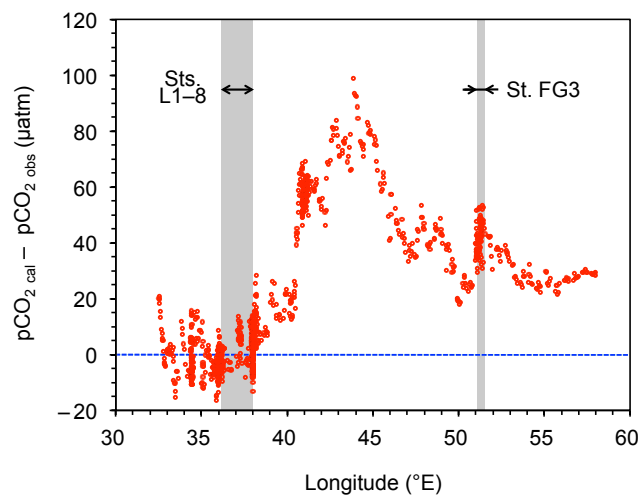


**Figure 10.** Longitudinal distribution of the difference between calculated and observed  $p\text{CO}_2$ . Calculated  $p\text{CO}_2$  was computed from  $n\text{-DIC}_{(w)}$  and  $n\text{-TA}_{(w)}$  at the observed SST.

fect was dominant at  $32$ – $40^{\circ}\text{E}$ . The positive excursion of this  $p\text{CO}_2$  differential at  $40$ – $58^{\circ}\text{E}$  would be explained by biological productivity (Fig. 2b), which would reduce  $p\text{CO}_{2\text{obs}}$ . The similarities of the longitudinal distributions of  $p\text{CO}_2$  and chlorophyll  $a$  concentrations are consistent with these relationships (Figs. 2b and 10).

The  $\text{CO}_2$  flux between air and water ( $F_{\text{CO}_2(a-w)}$ ) also changed in synchrony with the variations of surface-water  $p\text{CO}_2$  ( $p\text{CO}_{2w}$ ) and sea ice concentration (Fig. 9). In Eq. (7), we treated sea ice as a barrier to  $\text{CO}_2$  exchange between air and sea. Therefore,  $F_{\text{CO}_2(a-w)}$  was defined as zero until sea ice concentration decreased in late December. During ice retreat, surface water was an early  $\text{CO}_2$  source to the atmosphere because of its supersaturation with respect to the atmosphere (Fig. 9a). Therefore,  $F_{\text{CO}_2(a-w)}$  reached up to  $+0.9 \text{ mmol C m}^{-2} \text{ day}^{-1}$  at the beginning of January 2006 (Fig. 9b). Subsequently, photosynthesis and carbonate crystals in sea ice meltwater would lower  $p\text{CO}_{2w}$  to the point that the water became a  $\text{CO}_2$  sink (Fig. 9a). Our  $F_{\text{CO}_2(a-w)}$  ( $0.0$  to  $+0.9 \text{ mmol C m}^{-2} \text{ day}^{-1}$ ) falls within the range ( $-8.2$  to  $+7.2 \text{ mmol C m}^{-2} \text{ day}^{-1}$ ) reported in previous studies in the SIZ (Bakker et al., 1997; Metzl et al., 1999, 2006; Chierici et al., 2004; Nakaoka et al., 2009).

Although our estimate treated sea ice as impermeable to  $\text{CO}_2$  exchange, recent studies have proposed that  $\text{CO}_2$  exchange occurs through sea ice (Semiletov et al., 2004; Delille, 2006; Nomura et al., 2006, 2010a, b, 2013a; Zemmelink et al., 2006; Loose et al., 2009; Miller et al., 2011; Geilfus et al., 2012). Early during the period of ice growth,  $p\text{CO}_2$  of brine in sea ice attains supersaturation with respect to the atmosphere with decreasing temperature and increasing salinity (e.g., Papadimitriou et al., 2003). Thus, brine channels can emit  $\text{CO}_2$  to the overlying air and, if the ice

**Table 2.** Contributions of temperature ( $(\Delta p\text{CO}_{2\text{w}}) T$ ), air–sea flux ( $(\Delta p\text{CO}_{2\text{w}}) F$ ), biological production ( $(\Delta p\text{CO}_{2\text{w}}) B$ ) and residual mechanisms ( $(\Delta p\text{CO}_{2\text{w}}) R$ ) to the winter-to-summer evolution of surface-water  $p\text{CO}_2$  ( $\Delta p\text{CO}_{2\text{w}(w)\text{to}(s)}$ ) for each station.

Station	$\Delta p\text{CO}_{2\text{w}(w)\text{to}(s)}$	$(\Delta p\text{CO}_{2\text{w}}) T$	$(\Delta p\text{CO}_{2\text{w}}) F$	$(\Delta p\text{CO}_{2\text{w}}) B$	$(\Delta p\text{CO}_{2\text{w}}) R$
L1	42.0	38.6	−0.1	−9.2	12.7
L2	38.3	34.7	−0.1	*	3.7
L3	39.8	34.7	−0.2	−6.3	11.6
L4	30.1	30.4	0.0	*	−0.3
L5	39.7	39.6	−0.2	*	0.3
L6	40.7	40.9	−0.6	−5.2	5.6
L7	42.0	40.9	−0.7	*	1.8
L8	15.4	33.9	0.0	*	−18.5
FG3	−13.2	24.3	0.1	−23.8	−13.8

\* No data due to no significant difference in  $n$ -DIC between the surface and the upper part of the TML for NCP calculation. NCP was  $2.5 \text{ g C m}^{-2}$  for station L1,  $1.7 \text{ g C m}^{-2}$  for station L3,  $1.5 \text{ g C m}^{-2}$  for station L6 and  $13.5 \text{ g C m}^{-2}$  for station FG3.

permeability is sufficiently high, to the overlying atmosphere (Delille, 2006; Nomura et al., 2006, 2010b; Loose et al., 2009; Miller et al., 2011a; Geilfus et al., 2012). Furthermore, during the period of ice melt, sea ice brine may take up atmospheric  $\text{CO}_2$  because  $p\text{CO}_2$  of brine becomes undersaturated with respect to the atmosphere due to algal productivity and dilution by meltwater (Semiletov et al., 2004; Delille, 2006; Zemmeling et al., 2006; Nomura et al., 2010a, 2013a). We incorporated this component as follows, using recent observations of Antarctic and Arctic sea ice (Nomura et al., 2013a):

$$F_{\text{CO}_2(\text{a-w})} + F_{\text{CO}_2(\text{a-i})} = k \cdot s(p\text{CO}_{2\text{a}} - p\text{CO}_{2\text{w}}) \cdot (100 - A)/100 + F_i \cdot A/100, \quad (11)$$

where  $F_{\text{CO}_2(\text{a-w})}$  and  $F_{\text{CO}_2(\text{a-i})}$  are, respectively, the  $\text{CO}_2$  flux between air and water and air and ice including sea ice concentration.  $F_{\text{CO}_2(\text{a-i})}$  is the  $\text{CO}_2$  flux measured over the sea ice, and it was added to Eq. (7) in order to form Eq. (11). Because sea ice melts and becomes flooded during seasonal warming even while sea ice concentration is still high, we used the value  $-1.1 \pm 0.9 \text{ mmol C m}^{-2} \text{ day}^{-1}$  for  $F_i$ , taken from direct measurements by the chamber technique over the melting and flooded sea ice surface (Nomura et al., 2013a). The formation of the surface flooded (slush or gap) layer likely occurs frequently in melting Antarctic sea ice (Haas et al., 2001; Kattner et al., 2004; Ackley et al., 2008; Zemmeling et al., 2008; Papadimitriou et al., 2009; Nomura et al., 2012, 2013b). Snow accumulation over sea ice and the formation of superimposed ice leads to the formation of a slush layer below sea level (Haas et al., 2001).  $F_i$  ( $-1.1 \pm 0.9 \text{ mmol C m}^{-2} \text{ day}^{-1}$ ) was within the range ( $-5.2$  to  $+0.9 \text{ mmol C m}^{-2} \text{ day}^{-1}$ ) reported by previous studies using the chamber method (Delille, 2006; Nomura et al., 2010a, 2010b; Geilfus et al., 2012). Our calculations show that the  $\text{CO}_2$  flux between air and ice ( $F_i$ ) was dominant until the sea ice retreat beginning in December, when the positive  $\text{CO}_2$  flux between air and water overcame it and the net  $\text{CO}_2$  flux to the air became positive, reaching

about  $+0.8 \text{ mmol C m}^{-2} \text{ day}^{-1}$  after the sea ice disappeared (Fig. 9b).

It has been argued that leads, cracks and polynyas within the sea ice area are hot spots for gas exchange between the air and surface water (Zemmeling et al., 2008; Else et al., 2013; Steiner et al., 2013). However, the formation of surface melt ponds (Semiletov et al., 2004) and carbon uptake by algae within them (Lee et al., 2012) can also contribute to  $\text{CO}_2$  uptake. Even without considering meltwater, the presence of snow on sea ice also affects the  $\text{CO}_2$  flux (Nomura et al., 2010a, 2013a). For an accurate calculation of  $\text{CO}_2$  flux in the SIZ, it is clear that, in addition to the open ocean surface, ice areas are influential in the carbon and biogeochemical cycles of polar seas.

## 5 Conclusions

The results of this study shed light on  $\text{CO}_2$  dynamics and flux during the winter-to-summer transition in the SIZ. For the surface-water  $p\text{CO}_2$ , we demonstrated that  $p\text{CO}_2$  variations have a thermodynamic origin before the onset of active biological productivity. With regard to the  $\text{CO}_2$  flux, it is not yet certain whether the SIZ acts as a  $\text{CO}_2$  sink or source relative to the atmosphere throughout this season. This study evaluated the air–sea  $\text{CO}_2$  flux (including the air–ice  $\text{CO}_2$  flux) as negative in winter, indicating a  $\text{CO}_2$  sink (Fig. 9a). Although sea ice blocks the direct exchange of  $\text{CO}_2$  between the ocean and the atmosphere,  $p\text{CO}_2$  in the water under the ice ( $349.9 \mu\text{atm}$ ) is low with respect to the atmosphere (Fig. 9a), suggesting that, in addition to sea ice, water in the SIZ is a potential  $\text{CO}_2$  sink in winter (Nomura et al., 2013a). Ishii et al. (2002), however, reported that  $p\text{CO}_2$  in surface water ( $390 \mu\text{atm}$ ) is high in winter with respect to the atmosphere near our study area and that  $\text{CO}_2$  could enter the atmosphere (indicating a  $\text{CO}_2$  source) through ice-free regions, such as polynyas and leads. Further studies are needed to address these conflicting findings.

**Acknowledgements.** We thank the crew of R/V *Umitaka-Maru* and cruise members for their support in conducting the field work. This work was partly supported by the Japan Society for the Promotion of Science (23241002) and the National Institute of Polar Research.

Edited by: Laurent Bopp

## References

- Ackley, S. F., Lewis, M. J., Fritsen, C. H., and Xie, H.: Internal melting in Antarctic sea ice: Development of “gap layers”, *Geophys. Res. Lett.*, 35, L11503, doi:10.1029/2008GL033644, 2008.
- Anderson, L. A. and Sarmiento, J. L.: Redfield ratios of remineralization determined by nutrient data analysis, *Global Biogeochem. Cy.*, 8, 65–80, 1994.
- Bakker, D. C. E., de Baar, H. J. W., and Bathmann, U. V.: Changes of carbon dioxide in surface waters during spring in the Southern Ocean, *Deep-Sea Res. II*, 44, 91–127, 1997.
- Bakker, D. C. E., Hoppema, M., Schröder, M., Geibert, W., and de Baar, H. J. W.: A rapid transition from ice covered  $\text{CO}_2$ -rich waters to a biologically mediated  $\text{CO}_2$  sink in the eastern Weddell Gyre, *Biogeosciences*, 5, 1373–1386, doi:10.5194/bg-5-1373-2008, 2008.
- Bellerby, R. G. J., Hoppema, M., Fahrbach, E., De Baar, H. J. W., and Stoll, M. H. C.: Interannual controls on Weddell Sea surface water  $f\text{CO}_2$  during the autumn-winter transition phase, *Deep-Sea Res. I*, 51, 793–808, 2004.
- Cannizzaro, J. P., Hu, C., Carder, K. L., Kelble, C. R., Melo, N., Johns, E. M., Vargo, G. A., and Heil, C. A.: On the accuracy of SeaWiFS ocean color data products on the West Florida Shelf, *J. Coast. Res.* 29, 6, 1257–1272, doi:10.2112/JCOASTRES-D-12-00223.1, 2013.
- Chierici, M., Fransson, A., Turner, D. R., Pakhomov, E. A., and Froneman, P. W.: Variability in pH,  $f\text{CO}_2$ , Oxygen and flux of  $\text{CO}_2$  in the surface water along a transect in the Atlantic sector of the Southern Ocean, *Deep-Sea Res. II*, 51, 2773–2787, 2004.
- Copin-Montegut, C.: A new formula for the effect of temperature on the partial pressure of  $\text{CO}_2$  in seawater, *Mar. Chem.*, 25, 29–37, 1988 (Correction, *Mar. Chem.*, 27, 143–144, 1989).
- Culberson, C., Pytkowicz, R. M., and Hawley, J. E.: Seawater alkalinity determination by the pH method, *J. Mar. Res.*, 28, 15–21, 1970.
- Delille, B.: Inorganic carbon dynamics and air-ice-sea  $\text{CO}_2$  fluxes in the open and coastal waters of the Southern Ocean, Ph. D. thesis, Univ. of Liège, Liège, Belgium, 1–297, 2006.
- Dickson, A. G.: Thermodynamics of the dissociation of boric acid in synthetic seawater from 273.15 to 318.15 K, *Deep-Sea Res. I*, 37, 755–766, 1990.
- Dickson, A. G. and Millero, F. J.: A comparison of the equilibrium constants for the dissociation of carbonic acid in seawater media, *Deep-Sea Res.*, 34, 1733–1743, 1987.
- Dieckmann, G. S., Nehrke, G., Papadimitriou, S., Göttlicher, J., Steininger, R., Kennedy, H., Wolf-Gladrow, D., and Thomas, D. N.: Calcium carbonate as ikaite crystals in Antarctic sea ice, *Geophys. Res. Lett.*, 35, L08501, doi:10.1029/2008GL033540, 2008.
- Edson, J. B., Fairall, C. W., Bariteau, L., Zappa, C. J., Cifuentes-Lorenzen, A., McGillis, W. R., Pezoa, S., Hare, J. E., and Helmig, D.: Direct covariance measurement of  $\text{CO}_2$  gas transfer velocity during the 2008 Southern Ocean Gas Exchange Experiment: Wind speed dependency, *J. Geophys. Res.* 116, C00F10, doi:10.1029/2011JC007022, 2011.
- Else, B. G. T., Papakyriakou, T. N., Asplin, M. G., Barber, D. G., Galley, R. J., Miller, L. A., and Mucci, A.: Annual Cycle of Air-Sea  $\text{CO}_2$  Exchange in an Arctic Polynya Region, *Global Biogeochem. Cy.*, 27, 388–398, 2013.
- Fransson, A., Chierici, M., Yager, P. L., and Smith Jr., W. O.: Antarctic sea ice carbon dioxide system and controls, *J. Geophys. Res.*, 116, C12035, doi:10.1029/2010JC006844, 2011.
- Geilfus, N.-X., Carnat, G., Papakyriakou, T., Tison, J.-L., Else, B., Thomas, H., Shadwick, E., and Delille, B.: Dynamics of  $p\text{CO}_2$  and related air-ice  $\text{CO}_2$  fluxes in the Arctic coastal zone (Amundsen Gulf, Beaufort Sea), *J. Geophys. Res.*, 117, C00G10, doi:10.1029/2011JC007118, 2012.
- Gibson, J. A. E. and Trull, T. W.: Annual cycle of  $f\text{CO}_2$  under sea-ice and in open water in Prydz Bay, East Antarctica, *Mar. Chem.*, 66, 187–200, 1999.
- Haas, C., Thomas, D. N., and Bareiss, J.: Surface properties and processes of perennial Antarctic sea ice in summer, *J. Glaciol.*, 47, 613–625, 2001.
- Hales, B. and Takahashi, T.: High-resolution biogeochemical investigation of the Ross Sea, Antarctica, during the AESOPS (US JGOFS) Program, *Global Biogeochem. Cy.*, 18, GB3006, doi:10.1029/2003GB002165, 2004.
- Ho, D. T., Law, C. S., Smith, M. J., Schlosser, P., Harvey, M., and Hill, P.: Measurements of air-sea gas exchange at high wind speeds in the Southern Ocean: Implications for global parameterizations, *Geophys. Res. Lett.*, 33, L16611, doi:10.1029/2006GL026817, 2006.
- Hoppema, M. and Goeyens, L.: Redfield behavior of carbon, nitrogen, and phosphorus depletions in Antarctic surface water, *Limnol. Oceanogr.*, 44, 220–224, 1999.
- Hoppema, M., Fahrbach, E., Schröder, M., Wisotzki, A., and de Baar, H. J. W.: Winter-summer difference of carbon dioxide and oxygen in the Weddell Sea surface layer, *Mar. Chem.*, 51, 177–192, 1995.
- Inoue, H. Y., Ishii, M., Matsueda, H., Saito, S., Midorikawa, T., and Nemoto, K.: Partial pressure of  $\text{CO}_2$  in surface waters of the Pacific during 1968 to 1970: re-evaluation and comparison of data, *Tellus B*, 830–848, 1999.
- Inoue, H. Y. and Ishii, M.: Variations and trends of  $\text{CO}_2$  in the surface seawater in the Southern Ocean south of Australia between 1969 and 2002, *Tellus B*, 58–69, 2005.
- IPCC, Climate change, 2007: the physical science basis. In: Solomon, edited by: S., Quin, D., Manning, M., Chen, Z., Marquis, M., Averyt, K.B., Tignor, M., and Miller, H. L., Contribution of Working Group I of the Fourth Assessment Report of the Intergovernmental Panel on Climate Change, Cambridge University Press, Cambridge, United Kingdom and New York, NY, USA, 996 pp., 2007.
- Ishii, M., Inoue, H. Y., Matsueda, H., and Tanoue, E.: Close coupling between seasonal biological production and dynamics of dissolved inorganic carbon in the Indian Ocean sector and the western Pacific Ocean sector of the Antarctic Ocean, *Deep-Sea Res. I*, 45, 1187–1209, 1998.
- Ishii, M., Inoue, H. Y., and Matsueda, H.: Net community production in the marginal ice zone and its importance for the variability of the oceanic  $p\text{CO}_2$  in the Southern Ocean south of Australia, *Deep-Sea Res. II*, 49, 1691–1706, 2002.

- Jabaud-Jan, A., Metzl, N., Brunet, C., Poisson, A., and Schauer, B.: Interannual variability of the carbon dioxide system in the southern Indian Ocean (20–60° S): the impact of a warm anomaly in austral summer 1998, *Global Biogeochem. Cy.*, 18, B1042, doi:10.1029/2002GB002017, 2004.
- Johnson, K. M., Körtzinger, A., Mintrop, L., Duinker, J. C., and Wallace, D. W. R.: Coulometric total carbon dioxide analysis for marine studies: measurements and internal consistency of underway  $\text{TCO}_2$  concentrations, *Mar. Chem.*, 67, 123–144, 1999.
- Kalnay, E., Kanamitsu, M., Kistler, R., Collins, W., Deaven, D., Gandin, L., Iredell, M., Saha, S., White, G., Woollen, J., Zhu, Y., Leetmaa, A., Reynolds, R., Chelliah, M., Ebisuzaki, W., Higgins, W., Janowiak, J., Mo, K. C., Ropelewski, C., Wang, J., Jenne, R., and Joseph, D.: The NCEP/NCAR 40-Year Reanalysis Project, *Bull. Amer. Meteor. Soc.*, 77, 437–471, 1996.
- Kattner, G., Thomas, D. N., Haas, C., Kennedy, H., and Dieckmann, G. S.: Surface ice and gap layers in Antarctic sea ice: highly productive habitats, *Mar. Ecol. Prog. Ser.*, 277, 1–12, 2004.
- Lee, S. H., Stockwell, D. A., Joo, H.-M., Son, Y., Kang, C.-K., and Whitley, T. E. E.: Phytoplankton production from melting ponds on Arctic sea ice, *J. Geophys. Res.*, 117, C4, doi:10.1029/2011JC007717, 2012.
- Lewis, E. and Wallace, D. W. R.: Program Developed for  $\text{CO}_2$  System Calculations, ORNL/CDIAC-105, Carbon Dioxide Information Analysis Center, Oak Ridge National Laboratory, US Department of Energy, Oak Ridge, TN, available at: <http://cdiac.esd.ornl.gov/oceans/co2rprt.html>, 1998.
- Loose, B., McGillis, W. R., Schlosser, P., Perovich, D., and Takahashi, T.: Effects of freezing, growth, and ice cover on gas transport processes in laboratory seawater experiments, *Geophys. Res. Lett.*, 36, doi:10.1029/2008GL036318, 2009.
- McNeil, B. I., Metzl, N., Key, R. M., Matear, R. J., and Corbière, A.: An empirical estimate of the Southern Ocean air–sea  $\text{CO}_2$  flux, *Global Biogeochem. Cy.*, 21, GB3011, doi:10.1029/2007GB002991, 2007.
- Mehrbach, C., Culbertson, C.H., Hawley, J. E., and Pytkowicz, R. M.: Measurement of the apparent dissociation constants of carbonic acid in seawater at atmospheric pressure, *Limnol. Oceanogr.*, 18, 897–907, 1973.
- Metzl, N., Tilbrook, B., and Poisson, A.: The annual  $f\text{CO}_2$  cycle and the air–sea  $\text{CO}_2$  fluxes in the sub-Antarctic Ocean, *Tellus B*, 51, 849–861, 1999.
- Metzl, N., Brunet, C., Jabaud-Jan, A., Poisson, A., and Schauer, B.: Summer and winter air–sea  $\text{CO}_2$  fluxes in the Southern Ocean, *Deep-Sea Res. I*, 53, 1548–1563, 2006.
- Miller, L. A., Papakyriakou, T. N., Collins, R. E., Deming, J. W., Ehn, J. K., Macdonald, R. W., Mucci, A., Owens, O., Raudsepp, M., and Sutherland, N.: Carbon dynamics in sea ice: A winter flux time series, *J. Geophys. Res.*, 116, C02028, doi:10.1029/2009JC006058, 2011.
- Moore, J. K. and Abbott, M. R.: Phytoplankton chlorophyll distributions and primary production in the Southern Ocean, *J. Geophys. Res.*, 105, 28709–28772, 2000.
- Nakaoka, S., Nakazawa, T., Yoshikawa-Inoue, H., Aoki, S., Hashida, G., Ishii, M., Yamanouchi, T., Odate, T., and Fukuchi, M.: Variations of oceanic  $p\text{CO}_2$  and air–sea  $\text{CO}_2$  flux in the eastern Indian sector of the Southern Ocean for the austral summer of 2001–2002, *Geophys. Res. Lett.*, 36, L14610, doi:10.1029/2009GL038467, 2009.
- Nomura, D., Inoue, H. Y., and Toyota, T.: The effect of sea-ice growth on air–sea  $\text{CO}_2$  flux in a tank experiment, *Tellus B*, 58, 418–426, 2006.
- Nomura, D., Inoue, H. Y., Toyota, T., and Shirasawa, K.: Effects of snow, snowmelting and refreezing processes on air–sea-ice  $\text{CO}_2$  flux, *J. Glaciol.*, 56, 262–270, 2010a.
- Nomura, D., Eicken, H., Gradinger, R., and Shirasawa, K.: Rapid physically driven inversion of the air–sea ice  $\text{CO}_2$  flux in the seasonal landfast ice off Barrow, Alaska after onset of surface melt, *Cont. Shelf Res.*, 30, 1998–2004, 2010b.
- Nomura, D., Koga, S., Kasamatsu, N., Shinagawa, H., Simizu, D., Wada, M., and Fukuchi, M.: Direct measurements of DMS flux from Antarctic fast sea ice to the atmosphere by a chamber technique, *J. Geophys. Res.*, 117, C04011, doi:10.1029/2010JC006755, 2012.
- Nomura, D., Granskog, M. A., Assmy, P., Simizu, D., and Hashida, G.: Arctic and Antarctic sea ice acts as a sink for atmospheric  $\text{CO}_2$  during periods of snow melt and surface flooding, *J. Geophys. Res.*, 118, 6511–6524, 2013a.
- Nomura, D., Assmy, P., Nehrke, G., Granskog, M. A., Fischer, M., Dieckmann, G. S., Fransson, A., Hu, Y., and Schnetger, B.: Characterization of ikaite ( $\text{CaCO}_3 \cdot 6\text{H}_2\text{O}$ ) crystals in first-year Arctic sea ice north of Svalbard, *Ann. Glaciol.*, 54, 62, 125–131, doi:10.3189/2013AoG62A034, 2013b.
- Papadimitriou, S., Kennedy, H., Kattner, G., Dieckmann, G. S., and Thomas, D. N.: Experimental evidence for carbonate precipitation and  $\text{CO}_2$  degassing during sea ice formation, *Geochim. Cosmochim. Ac.*, 68, 1749–1761, 2003.
- Papadimitriou, S., Thomas, D. N., Kennedy, H., Kuosa, H., and Dieckmann, G. S.: Inorganic carbon removal and isotopic enrichment in Antarctic sea ice gap layers during early austral summer, *Mar. Ecol. Prog. Ser.*, 386, 15–27, 2009.
- Parsons, T. R., Takahashi, M., and Hargrave, B.: *Biological Oceanographic Processes*, 3, 330 pp., Pergamon, Oxford, UK, 1984.
- Pondaven, P., Ragueneau, O., Tréguer, P., Hauvespre, A., Dezileau, L., and Reyss, J. L.: Resolving the “opal paradox” in the Southern Ocean, *Nature*, 405, 168–172, 2000.
- Reynolds, R. W., Rayner, N. A., Smith, T. M., Stokes, D. C., and Wang, W.: An improved in situ and satellite SST analysis for climate, *J. Clim.*, 15, 1609–1625, 2002.
- Rintoul, S. R. and Bullister, J. L.: A late winter hydrographic section from Tasmania to Antarctica, *Deep-Sea Res. I*, 46, 1417–1454, 1999.
- Rubin, S. I., Takahashi, T., Chipman, D. W., and Goddard, J. G.: Primary productivity and nutrient utilization ratios in the Pacific sector of the Southern Ocean based on seasonal changes in seawater chemistry, *Deep-Sea Res. I*, 45, 1211–1234, 1998.
- Rysgaard, S., Glud, R. N., Sejr, M. K., Bendtsen, J., and Christensen, P. B.: Inorganic carbon transport during sea ice growth and decay: a carbon pump in polar seas, *J. Geophys. Res.*, 112, C03016, doi:10.1029/2006JC003572, 2007.
- Rysgaard, S., Søgaard, D. H., Cooper, M., Pućko, M., Lennert, K., Papakyriakou, T. N., Wang, F., Geilfus, N. X., Glud, R. N., Ehn, J., McGinnis, D. F., Attard, K., Sievers, J., Deming, J. W., and Barber, D.: Ikaite crystal distribution in winter sea ice and implications for  $\text{CO}_2$  system dynamics, *The Cryosphere*, 7, 707–718, doi:10.5194/tc-7-707-2013, 2013.
- Sabine, C. L. and Key, R. M.: Controls on  $f\text{CO}_2$  in the South Pacific, *Mar. Chem.*, 60, 95–110, 1998.

- Semiletov, I., Makshtas, S., Akasofu, S., and Andreas, E. L.: Atmospheric  $\text{CO}_2$  balance: The role of Arctic sea ice, *Geophys. Res. Lett.*, 31, doi:10.1029/2003GL017996, 2004.
- Shim, J., Kang, Y. C., Kim, D., and Choi, S.: Distribution of net community production and surface  $p\text{CO}_2$  in the Scotia Sea, Antarctica, during austral spring 2001, *Mar. Chem.*, 101, 68–84, 2006.
- Steiner, N., Lee, W. G., and Christian, J. R.: Enhanced gas fluxes in small sea ice leads and cracks: Effects on  $\text{CO}_2$  exchange and ocean acidification, *J. Geophys. Res.*, 118, 1195–1205, 2013.
- Stoll, M. H. C., de Baar, H. J. W., Hoppema, M., and Fahrbach, E.: New early winter  $f\text{CO}_2$  data reveal continuous uptake of  $\text{CO}_2$  by the Weddell Sea, *Tellus B*, 51, 679–687, 1999.
- Suzuki, R. and Ishimaru, T.: An improved method for the determination of phytoplankton chlorophyll using N, N-dimethylformamide, *J. Oceanogr. Soc. Jpn.*, 46, 190–194, doi:10.1007/BF02125580, 1990.
- Sweeney, C.: The annual cycle of surface  $\text{CO}_2$  and  $\text{O}_2$  in the Ross Sea: a model for gas exchange on the continental shelves of Antarctica, in: *Biogeochemistry of the Ross Sea*, edited by: DiTullio, G. R., and Dunbar, R. B., *Antarct. Res. Ser.*, 78, 295–312, 2003.
- Sweeney, C., Smith, W. O., Hales, B., Bidigare, R. R., Carlson, C. A., Codispoti, L. A., Gordon, L. I., Hansell, D., Millero, F. J., Park, M.-O. K., and Takahashi, T.: Nutrient and carbon removal ratios and fluxes in the Ross Sea, Antarctica, *Deep-Sea Res. II*, 47, 3395–3421, 2000.
- Takahashi, T., Olafsson, J., Goddard, J. G., Chipman, D. W., and Sutherland, S. C.: Seasonal variations of  $\text{CO}_2$  and nutrients in the high-latitude surface oceans: a comparative study, *Global Biogeochem. Cy.*, 7, 843–878, 1993.
- Takahashi, T., Sutherland, S. C., Sweeney, C., Poisson, A., Metzl, N., Tilbrook, B., Nates, N., Wanninkhof, R., Feely, R. A., Sabine, C., Olafsson, J., and Nojiri, Y.: Global sea-air  $\text{CO}_2$  flux based on climatological surface ocean  $p\text{CO}_2$  and seasonal biological and temperature effects, *Deep-Sea Res.*, II, 49, 1601–1622, 2002.
- Takahashi, T., Sutherland, S. C., Wanninkhof, R., Sweeney, C., Feely, R. A., Chipman, D. W., Hales, B., Friederich, G., Chavez, F., Sabine, C., Watson, A., Bakker, D. C. E., Schuster, U., Metzl, N., Yoshikawa-Inoue, H., Ishii, M., Midorikawa, T., Nojiri, Y., Körtzinger, A., Steinhoff, T., Hoppema, M., Olafsson, J., Arnarson, T. S., Tilbrook, B., Johannessen, T., Olsen, A., Bellerby, R., Wong, C. S., Delille, B., Bates, N. R., and de Baar, H. J. W.: Climatological mean and decadal change in surface ocean  $p\text{CO}_2$ , and net sea-air  $\text{CO}_2$  flux over the global oceans, *Deep-Sea Res. II*, 56, 554–577, 2009.
- Takahashi, T., Sweeney, C., Hales, B., Chipman, D. W., Newberger, T., Goddard, J. G., Iannuzzi, R. A., and Sutherland, S. C.: The changing carbon cycle in the Southern Ocean, *Oceanogr.*, 25, 26–37, 2012.
- Tomczak, M. and Liefvink, S.: Interannual variations of water mass volumes in the Southern Ocean, *J. Atmos. Ocean Sci.*, 10, 31–42, 2005, <http://www.ocean-sci.net/10/31/2005/>.
- Wakita, M., Watanebe, W. Y., Watanebe, S., and Noriki, S.: Oceanic uptake rate of anthropogenic  $\text{CO}_2$  in a subpolar marginal sea: the Sea of Okhotsk, *Geophys. Res. Lett.*, 30, doi:10.1029/2003GL018057, 2003.
- Wanninkhof, R.: Relationship between wind speed and gas exchange over the ocean, *J. Geophys. Res.*, 97, 7373–7382, 1992.
- Weiss, R. F.: Carbon dioxide in water and seawater: the solubility of a non-ideal gas, *Mar. Chem.*, 2, 203–205, 1974.
- Zeebe R. E. and Wolf-Gladrow, D.:  $\text{CO}_2$  in seawater: equilibrium, kinetics, isotopes (Elsevier Oceanogr. Ser. 65), Elsevier, Amsterdam, 346 pp., 2001.
- Zemmelink, H. J., Delille, B., Tison, J.-L., Hints, E. J., Houghton, L., and Dacey, J. W. H.:  $\text{CO}_2$  deposition over the multi-year ice of the western Weddell Sea, *Geophys. Res. Lett.*, 33, L13606, doi:10.1029/2006GL026320, 2006.
- Zemmelink, H. J., Houghton, L., Dacey, J. W. H., Stefels, J., Koch, B. P., Schroder, M., Wisotzki, A., Scheltz, A., Thomas, D. N., Papadimitriou, S., Kennedy, H., Kuosa, H., and Dittmar, T.: Stratification and the distribution of phytoplankton, nutrients, inorganic carbon and sulfur in the surface waters of Weddell Sea leads, *Deep-Sea Res. II*, 55, 988–999, 2008.